

Determination of Vitality from A Non-Invasive Biomedical Measurement for Use in Fingerprint Scanners

Reza Derakhshani*, MSEE
Graduate Research Assistant
Department of Computer Science and Electrical Engineering
West Virginia University
P.O.Box 6109
Morgantown, WV, 26506-6109
Phone: (304) 293 0405 ext. 2030
Fax: (304) 293 8602
E-mail: reza@csee.wvu.edu

Stephanie A.C. Schuckers, PhD
Assistant Professor
Department of Computer Science and Electrical Engineering
West Virginia University
P.O.Box 6109
Morgantown, WV, 26506-6109
Phone: (304) 293 0405 ext. 2519
Fax: (304) 293 8602
E-mail: scaswell@csee.wvu.edu

Larry A. Hornak, PhD
Associate Professor
Department of Computer Science and Electrical Engineering
West Virginia University
P.O.Box 6109
Morgantown, WV, 26506-6109
Phone: (304) 293 0405 ext. 2515
Fax: (304) 293 8602
E-mail: lah@msrc.wvu.edu

Lawrence O'Gorman, PhD
Avaya Labs, Room 1B04
233 Mt. Airy Road
Basking Ridge, NJ 0792
Phone: (908) 696 5211
Fax: (908) 696 5102
E-mail: logorman@avaya.com

Abstract- Fingerprints are the oldest and most widely used biometrics for personal identification. Unfortunately, it is usually possible to deceive automatic fingerprint identification systems by presenting a well-duplicated synthetic or dismembered finger. This paper introduces one method to provide fingerprint vitality authentication in order to solve this problem. Detection of a perspiration pattern over the fingertip skin identifies the vitality of a fingerprint. Mapping the two-dimensional fingerprint images into one-dimensional signals, two ensembles of measures, namely static and dynamic measures, are derived for classification. Static patterns as well as temporal changes in dielectric mosaic structure of the skin, caused by perspiration, demonstrate themselves in these signals. Using these measures, this algorithm quantifies the sweating pattern and makes a final decision about vitality of the fingerprint by a neural network trained by examples.

Keywords- Fingerprints, Vitality, Biometrics, Neural networks, Capacitive scanners, Image processing.

1-Introduction

Personal identification is a very important issue in today's complex, mobile and electronically networked societies. Identification can be in the form of either verification (checking a person against his/her claimed identity) or identification (finding out who a person is by matching the acquired characteristics against a large database of enrollees). For proving one's identity, a unique characteristic should be offered. To solve the problem of lost, forgotten, or stolen keys, cards, and passwords, an identifying biological measure called a biometric can be used. The chosen physiological signatures must be universal, unique, and permanent. Among all biometrics, fingerprints are the oldest and most widely used [1].

Unfortunately, depending on the capturing technique, it is usually possible to fool automatic fingerprint identification systems by presenting a well-duplicated synthetic or dismembered finger. To solve this problem, this paper introduces a new method for determination of the liveness or vitality of a finger. The corner stone of this new method is detection of (active) perspiration as a sign of life.

2-Background

2-1 Fingerprints and Related Fraud

Fingerprints are unique for each individual and each fingerprint is formed through embryonic development stages. Since 1960s, automated fingerprint identification systems (AFIS)

have been widely deployed in law enforcement agencies [1]. Depending on capturing technique and device, it is usually possible to fool the device by presenting a well-duplicated synthetic finger or a cadaver finger in process of verification/identification. Some have suggested anti-spoofing measures based on physiologic features which may include measuring skin resistance, temperature, pulse oximetry (blood oxygen measured by absorption of near infrared light and red light), electrocardiogram, and/or other physiological vitality indicators [2]. These measurements have the disadvantage that they are bulky and expensive. An ideal anti-spoofing method should utilize measures that would not require existing systems to have additional hardware or major reconfigurations. Furthermore, some of the features are easy to spoof. For example, a spoof finger can be coated with a material with similar electrical resistance as skin or it can easily be warmed to 37° C to fool a temperature sensor.

2-2 The Skin

Human skin is composed of three main layers. The outmost layer houses 600 sweat glands per square inch. It also absorbs lipid-soluble substances [3,4]. Sweat, a dilute sodium chloride solution, is diffused on the surface of skin through small pores. Skin pores do not disappear, move, or spontaneously change over time. Our observations show that the pore-to-pore distance is approximately 0.5 mm over the fingertips. This agrees with Ashbaugh's model for pore frequency [5].

The most important electrical characteristics of skin are impedance and capacitance, where the skin can be modeled as a matrix of parallel resistors and capacitors. The electrical model of skin

shows a mosaic structure because of perspiring pores, since sweat has such high dielectric constant and electrical conductivity compared to the (drier) lipids that build the outer layer of skin [6,7,8,9]. Generally speaking, the dielectric constant of sweat is around 30 times higher than the lipid [6].

2-3 Fingerprint Scanner

Fingerprint scanners use different mechanisms for capturing the fingerprint, including ultrasonic imaging, pressure sensor arrays, optical imaging, and capacitive proximity sensor arrays. This research uses a scanner from the latter category. Capacitance sensors are composed of a 2-D array of capacitors, using standard CMOS processing (Figure 1) [10]. These sensors are exposed to direct fingertip contact. A thin but very tough and resistant dielectric (passivation) layer separates the touching surface from the integrated circuit. The sensing range is short and capacitance decreases sharply as the distance from the surface of the device to the finger increases [10], so these devices are most sensitive to the parts of the fingertip which touch the sensor, i.e. the (porous) ridges. Each sensor's measured capacitance is translated into a grayscale level in the corresponding bitmap image of the captured fingerprint through a special circuitry. If the skin in contact with the sensor is moist, then, because of very high dielectric constant of sweat, the underlying sensor will yield a much higher capacitance, resulting in a darker (saturated) spot on the captured image. This feature makes these scanners specifically suitable for detection of perspiration.

3- Methods and Materials

A Veridicom (Santa Clara, CA) FPS100 capacitive fingerprint scanner was used as the capturing device. It was connected via USB port to a 233 MHz Pentium-based personal computer. Software was provided with the fingerprint scanner for image capture. Matlab5 was used for all processing and computation.

The training and test set includes 18 sets of fingerprint images from live individuals, 18 from cadavers, and 18 from spoofs. The live sets are from eighteen different individuals mainly in the age group of 20-29. The eighteen spoof sets were developed from play dough using rubber-based casts. Approval to perform data collection for live and spoof fingerprints was obtained from the WVU Institutional Review Board (IRB) protocol HS # 14517. Cadaver work was covered under IRB protocol HS # 14239 and was performed at WVU Musculoskeletal Research Center.

Nine images were collected over 5 seconds for each sample. The first and last images were used in the pattern recognition algorithm.

4- Description of Physiologic Phenomenon

Inspection of live versus cadaver/spoof fingerprint scans produced the following observations:

1- In live fingers, perspiration starts from the pores, either completely covering them or leaving the pore as a dry dot in center of the sweating source. Typically the first fingerprint scan

will look "patchy" due to this process and has formed the basis of our *static* approach for classification (Figure 2).

2- Second, the sweat diffuses along the ridges in time, making the semi-dry regions between the pores moister or darker in the image. Unless the skin is extremely dry, the pore region remains saturated while the moisture (sweat) spreads towards drier parts (Figure 2). This fact, captured by comparing two fingerprint images within 5 seconds, forms the basis of our *dynamic* approach.

3- The perspiration process does not occur in cadaver or spoof fingers. Figures 3 and 4 are two scans with the same five second time separation from cadaver and spoof fingers for comparison.

As can be seen, the basis for our method is simple and straightforward. Live fingers, as opposed to cadaver or spoof, demonstrate a temporal change in moisture due to perspiration, and the fingerprint scanner is sensitive to this moisture. The challenge of an image processing algorithm is to quantify the sweating pattern. Furthermore, since this is a physiological phenomenon, this pattern will be variable across subjects, and will also depend on the initial moisture content of the skin.

5- The Algorithm

5-1 Overview

To quantify the perspiration phenomenon in the time sequence of images, an algorithm was developed to map a 2-dimensional fingerprint image to a "signal" which represents the gray level values along the ridges. The last image collected is used to determine the location of the ridges, since it usually has darker ridges and yields better quality. Variations in gray levels in the signal correspond to variations in moisture both statically (on one image) and dynamically (difference between first and last image). A Fourier transform of the signal is used to quantify the "static" variability in gray level along the ridges due to the pores and presence of perspiration. In particular, the algorithm focuses on frequencies corresponding to the spatial frequency of the pores. Secondly, dynamic features quantify the change in the local maximums and minimums in the ridge signal.

Below are the basic steps performed in the algorithm. More details will be given in the next section.

1- Capture a pair of consecutive fingerprints in five seconds. The image at time 0 will be called the first image and the second taken at time 5 seconds will be called the last.

2- Process the fingerprints to remove noise and device defects, using a noise reduction routine and median filter.

3- Obtain the binary version of the last image.

4- Thin the binary image so the ridges are only one pixel wide. Shift the result so that the resulting contours pass through the middle of the ridges.

5- Remove the Y connections so contours only consist of individual curves.

6- Erode two pixels from each to eliminate the extremes, and spurs. Throw away curves shorter than 15 pixels.

7- Use the curves obtained from step 6 as a mask, and convert the gray scales along them into signals for both the first and the last capture.

8- Calculate the FFT of first capture signal segments from step 7 and average. Calculate the total energy that corresponds to the spatial frequency of the pores. This measure is a *static* feature.

9- Connect the signals obtained in 7 for both the first and last captures and form a long signal which represents each fingerprint (C_1, C_2).

10- Detect the local maximums and minimums of first and last fingerprint signals.

11- Calculate a series of parameters (described later) quantifying the sweating process.

These measures are *dynamic* features.

12- Record the results and process the selected features.

13- Make a decision on vitality using a trained neural network using the features described above.

5-2 Detailed Description

1- Capture: An important point here is that the finger should not be moisture-saturated initially. The basis for this algorithm is detection of perspiration. If the skin is already very moist, the scanned image will be detected as a temporally stable fingerprint (steady state). If the finger is in such a state, one can rub his/her finger against a piece of cloth, before the capturing begins. The

first and last fingerprint images are captured 5 seconds apart, during which time perspiration occurs.

2- Pre-process: A program developed to clean up the image subtracts the permanent irregularities in the scanner by comparing it to a "blank" capture taken for each individual case. It also removes the background static by discarding those pixels that change only within 2% of the "blank" scan (Figure 5). Next, a 3x3 median filter is applied here to "cover" the white pixels in the middle of the pores. This also smoothes the image further and eliminates "salt & pepper" noise, if any.

3- Convert to binary: Next a software module transforms the image to binary (Figure 5).

4,5,6- Contour extraction: By thinning the binary image of the last capture (until the ridges' widths are shrunk to one pixel, using Matlab's bwmorph infinite 'thin'ing routine) fingerprint ridge paths are determined. However, since the result does not pass through the middle of the original ridges, a shift is necessary. Y-junctions are removed using a simple 3x3 non-overlapping neighbor operation. The results of these three steps can be seen in Figure 6, where the extracted curves are superimposed on the original fingerprint for visualization. Curves shorter than 15 pixels are discarded since the nominal pore-to-pore distance is around 0.5 mm, spanning almost 10 pixels. The final contours extracted from the last image are used as a mask for both the first and the last image to create signals corresponding to gray levels of the image on the contours.

7,8- Static measure (SM): The curves, which traverse through the middle of the ridges (Figure 6), cover varying gray levels in the fingerprint image. The peaks denote the moist (perspiring pore)

locations and the valleys show the dryer regions, usually between each two pores. For live fingerprints, the peak-to-peak distance is around 10 pixels (0.5 mm) which is in accord with (perspiring) pore-to-pore distance. The variations in the cadaver/spoof fingerprint signal do not correspond to a specific periodicity because they do not have evenly spaced perspiring pores (Figure 7). The main feature, which quantifies this, is the average Fourier transform of the signal segments from the first capture where the energy related to the typical pore spacing is used. A 256-point FFT is performed. Total energy is evaluated for a 8-24 pixel distance (for a pore spacing of 0.4 to 1.2mm) which takes into account the case of one missing pore with maximum spacing of 0.6mm. This corresponds to a spatial frequency range is between 11 and 33 (number of FFT points / spatial period). Before taking the FFT, in order to eliminate the spike around zero frequency, the DC of the signal (only for this specific calculation) is removed. The procedure can be mathematically expressed as:

$$SM = \sum_{k=11}^{33} f(k)^2$$

where $f(k) = \frac{\sum_{i=1}^n \left| \sum_{p=1}^{256} S_{li}^a(p) e^{-j2\pi(k-1)(p-1)/256} \right|}{n}$, $S_{li}^a = S_{li} - \text{mean}(S_{li})$

where n is total number of individual strings obtained in step 6 and S_{li} is the individual strings from the first image.

As will be seen in the results, this proves to be an excellent measure. Figure 8 gives the average FFT for the first image for live, cadaver, and spoof fingerprints. The energy for cadaver and spoof is very low compared to live. In addition, the energy for the last live fingerprint is smaller relative to the first capture. This is logical, since the swing of the signal decreases in time as the moisture is spread more evenly. The energy for the first image will be used as static feature. The results of static measure for live, cadaver, and spoof fingerprints are depicted in Figure 9.

9- Fingerprint signals: Individual strings are connected to form a long signal, which describes the gray levels of the contours passing through middle of the ridges. Figure 7 shows three (magnified) samples from portions of the signals extracted from a live, cadaver, and spoof fingerprint, respectively.

10,11- Dynamic Measures: The dynamic features are described below:

The general swing (local maximum minus local minimum) for the live fingerprint is usually larger than that of the spoof and cadaver. In addition, this swing is typically smaller for the last capture compared to first. It is hypothesized that starting with a dry live finger, moisture begins mainly around the pores creating peaks in the fingerprint ridge signal. Gradually the moisture spreads along the ridges and the total swing decreases in time. This trend is not present for spoof and cadaver fingerprint signals.

For live fingerprint signals, the maximums are fairly constant, but the minimums increase from first to last capture. It is hypothesized that the pixels near the pores are relatively saturated with perspiration while areas between the pores are still relatively dry. The only exception is when

in the finger is extremely dry so even the pore area is not saturated. Based on the above, four dynamic features are introduced:

Total swing ratio of first to last fingerprint signal (DM1): According to our hypothesis, the fluctuation of the live fingerprint signal should be more in the first capture when we have moist pores and drier regions in between the pores (and so higher peaks and lower valleys) compared to last fingerprint signal where the sweat has diffused into drier regions (and there are less variations in gray level). The results are shown in Figure 10 and Table 3. In mathematical terms, the first dynamic measure (DM1) is as follows:

$$DM1 = \frac{\sum_{i=1}^m |C_{1i} - C_{1i-1}|}{\sum_{i=1}^m |C_{2i} - C_{2i-1}|}$$

where C_{1i} and C_{2i} refer to the gray level signal points of the first and last capture respectively, and m is the length of the ridge signal. Note that m is the same for C_1 and C_2 (since the same mask was used for C_1 and C_2).

Min/Max growth ratio of first to last fingerprint signal (DM2): For the live fingerprint signal, the heights of the maximums do not increase as fast as the minimums (the perspiring pores are already saturated). So the average ratio of the maximum growth to minimum growth of first compared to last should be larger for the live fingerprint signal compared to cadaver and spoof. The results are shown in Figure 11 and Table 3. In mathematical terms, dynamic measure 2 (DM2) is as follows:

$$DM2 = \frac{\sum_j (C_{2j}^{\min} - C_{1j}^{\min})}{\sum_k (C_{2k}^{\max} - C_{1k}^{\max})}$$

where C_{1j}^{\min} and C_{2j}^{\min} are the local minimums for the first and last scan, respectively, and C_{1k}^{\max} and C_{2k}^{\max} are the local maximums. Location of minimums and maximums were determined from the second scan and applied to both.

Last-first fingerprint signal difference mean (DM3): When the first ridge signal (C_1) is subtracted from the last (C_2), the difference for a finger with no life is less than a finger that is perspiring quantifying a temporal pattern of moisture. This feature is helpful because there is a general darkening effect for cadaver fingers over time, which translates to a signal with a baseline shifting up while maintaining the same ac pattern. This baseline shift cancels out in the subtracting procedure. Figure 12 and Table 3 show the results. In mathematical terms, dynamic measure 3 (DM3) is as follows:

$$DM3 = \frac{\sum_{i=1}^m (C_{2i} - C_{1i})}{m}$$

m , C_{1i} , and C_{2i} are the same as in DM1.

Percentage change of standard deviations of first and last fingerprint signals (DM4): The last proposed measure in the dynamic ensemble is the percentage change in standard deviation of last and first fingerprint signals for each case. The rational behind it is similar to the others: if the

fluctuation of the ridge signal is decreasing around the mean (the change typical for live fingerprint signal), the fourth dynamic measure (DM4) will increase Figure 13 and Table 3 show the results. In mathematical terms,

$$DM4 = \frac{SD(C_1) - SD(C_2)}{SD(C_1)}$$

where SD is the standard deviation operator:

$$SD(C) = \sqrt{\frac{\sum_{i=1}^m (C_i - mean(C))^2}{m - 1}}$$

12,13- Classification: Classification can be performed based on each of the developed measures individually. The equal error rates (EER) are given in Table 3 [14]. False accept ratio (FAR) is defined as the percentage of cadaver or spoof fingerprints that are detected as live. False reject ratio (FRR) is defined as the percentage of live fingerprints that are detected as cadaver/spoof. The equal error rate is the result for the threshold which provides equal FAR and FRR. However, a decision based on a combination of static and four dynamic measures is able to give a much better classification.

6- Results

None of the developed features alone can separate live and cadaver/spoof fingerprints with 100% sensitivity and specificity (or no false acceptances and no false rejections). However, since the underlying mechanisms for static and dynamic measures are different, a combination of all these measures provides better precision than any of the individual measures. In this study, neural network is used for classification.

A back-propagation neural network (BPNN) is utilized in this work to separate live from cadaver/spoof fingerprints (Figure 14). BPNN uses gradient descent in conjunction with batch input-output training vectors for classification. Using the sigmoid nonlinear transfer function and bias, the BPNN is able to approximate any function with a finite number of discontinuities [11]. For convenience of training, bipolar targets (+1, -1) were chosen to denote live and cadaver/spoof, respectively. This three layer neural network constructs a mapping from the input space, i.e. dynamic and static measure outputs of each fingerprint pair, into an output space {dead, live} through a nested composition of nonlinearities [12]. Log-sigmoid was used for the hidden layer's transfer function. Linear and tan-sigmoid were tested for the output layer's transfer function. Using different initial random weights during many training sessions, the BPNNs with tan-sigmoid outperformed those with linear function in output layer, both in terms of training speed and accuracy on the test sets.

The five inputs to the neural network consist of the static measure and four dynamic measures. For this implementation, two-thirds of the data was used for training and one-third for testing. The network is trained using as many iterations (epochs) as needed until the sum of squared error (SSE) criteria, set at 0.02 in this study, is met (Figure 15). The output of the BPNN for the

training set is listed in Table 1, with the (ideal) set goals of +1 for live, -1 for cadaver/spoof. The output for the test set is listed in Table 2. Outputs (close to) +1 or -1 denote live or cadaver/spoof, respectively. When presented with the test inputs that it had never seen before, the BPNN classified all of the cases correctly.

7- Discussion and Future Work

The interesting finding during this research was that vitality of fingerprints can be determined from a new non-invasive method, detection of perspiration, by observing the fingerprint for a few seconds. It means that systems can become "spoof-proof" just by a simple software upgrade. Other proposed vitality measurements for fingerprint scanners require major hardware upgrades that will be bulky and expensive. One expanded method of using physiologic features is described in a US patent. This design is a multi-modal biometric identification system with a vitality tester [2]. The input to system comes from CCD camera (fingerprint scan), ECG electrodes (electrocardiogram of the claimant), LED and photo detector for pulse oximetry, and a temperature sensor. The system reads fingerprint for identification/verification (comparing to an enrollee) and uses skin temperature, pulse (both from ECG and optical readings, which should correlate), and oxygenation of blood for vitality measurement. If the fingerprint scan verifies the identity the claimant and if the second ensemble (vitality) readings fall into an acceptable range, then the claimant will be authenticated. In essence, the system is able to determine whether the live person is present while the fingerprint is being scanned. Automatic fingerprint identification system resistance to spoof fingers is performed by adding extra hardware which reads the vital signs from

the claimant's hands. Considering the accuracy of our proposed method, plus its ease of implementation without needing any additional hardware, one can argue that our method would be the preferred one.

On the other hand, because this algorithm expands upon the physiological phenomena of perspiration, it may experience difficulties in cases of perspiration disorders (finger too moist or dry) and other abnormal skin conditions. Nevertheless, one should note that many of these cases may also have problems when attempting to capture a usable fingerprint (because of abnormal moisture content). In the case of too moist, wiping the finger before scanning is performed is sufficient for this subject group.

. This is a subject to further investigation.

Another issue is the orthogonality of the derived features. Specifically, the dynamic features may not independently quantify the event. Future work will be to investigate the overlap and reduce their number or extract a new set of features from the fingerprint signals. Making a fair comparison of different feature sets using the neural net classifier is not an easy task, since the neural net does not train consistently even for the same input/target in different training sessions. However, an optimization would definitely lead to a more time efficient algorithm.

Another necessary improvement will be using a larger sample set both for training and for testing the algorithm. The sample set should include wider range of enrollees with different skin conditions in different climates and seasons as well as a more diverse background (race, age, etc). This is the subject of an ongoing study.

Another possible area of future work would be to decrease the time between the two captures, or to use more than two captures to derive more information. Tradeoffs between precision and speed of vitality verification will need to be addressed. For example, will the algorithm still

discriminate between a live vs. dead fingerprint if the time between the two captures is decreased to one second? More sophisticated algorithms maybe harder to spoof utilizing features which further quantify sweat diffusion speed and dispersion dynamism. These issues will be addressed during future work.

Finally, this algorithm and its future upgrades should be tested against spoofs which are made to simulate perspiration through artificial pores to evaluate the effort needed to spoof the algorithm.

As with all research, each study produces a new set of questions and potential improvements. In the area of security, complete security (without false rejects and accepts) will never be achieved permanently. The goal is to attempt to make spoofing of a system extremely difficult. This work introduces an additional requirement for fingerprint security through a successful method of vitality or liveness testing.

8- Conclusion

A new approach for detection of vitality through fingerprint examination in conjunction with capacitive scanners was introduced. This approach is based on detection of the sweating pattern from two consecutive fingerprints captured during 5 seconds. After mapping two-dimensional fingerprints into one-dimensional signals, two ensembles of measures, namely static and dynamic measures, are extracted from them. Classification is performed using a back propagation neural network trained by the example fingerprints. It quantifies the sweating pattern and makes the final decision about vitality of the fingerprint.

In conclusion, the method presented in here is a new measure for potential implementation in multi-modal biometrics systems. In addition to its accuracy, it is purely software based, so existing systems can be upgraded without any additional hardware.

This work has a US patent pending, provisional application submitted on October 7, 1999 [13].

Bibliography

[1] Lawrence O'Gorman, *Biometrics, Personal Identification in Networked Society*, Chapter 2 "Fingerprint Verification", edited by Anil Jain, Ruud Bolle, and Sharath Pankanti, , Kluwer Academic Publishers, 1999.

[2] David W. Osten, Hatim M. Carim, Michael R. Arneson, and Bradford L. Blan, "Biometric, Personal Authentication System"; United States Patent, # 5,719,950 patented on 2/17/1998.

[3] "Structure of the Skin", Columbia University College of P & S Complete Home Medical Guide, http://cpmcnet.columbia.edu/texts/guide/hmg28_0001.html .

[4] M.H.Ross, L.J. Romrell, and E.J. Reith, "The Integumentary System", From *Histology: A Text and Atlas*, 2nd Ed., Baltimore Williams and Wilkins, 1989, 347-349.

[5] Paul M. Quinton, "Sweating and Its Disorders", *Annual Reviews Med.*, Vol. 34, 1983, 429-452.

[6] Yuri A. Chizmadzhev, Andrey V. Indenborn, Peter I. Kuzmin, Sergey V. Galichenko, James C. Weaver, and Russel O. Potts, "Electrical Properties of Skin at Moderate Voltages: Contribution of Appendageal Macropores", *Biophysical Journal*, Vol. 74, February 1998, 843-856.

- [7] Dorin Panescu, Kevin P. Cohen, John G. Webster, and Robert A. Stratbucker, "The Mosaic Electrical Characteristics of the Skin", *IEEE Transactions on Biomedical Engineering*, Vol. 40, No. 5, May 1995, 434-439.
- [8] Dorin Panescu, John G. Webster, and Robert A. Stratbucker, "A Nonlinear Electrical-Thermal Model of the Skin", *IEEE Transactions on Biomedical Engineering*, Vol. 41, No. 7, July 1994, 672-679.
- [9] H.G.L. Coster, K.J. Kim, K. Dahlan, J.R. Smith and C.J.D. Fell, "Characterization of Ultrafiltration Membranes by Impedance Spectroscopy. I. Determination of the Separate Electrical Parameters and Porosity of the Skin and Sublayers", *Journal of Membrane Science*, Vol. 66, 1992, 19-26.
- [10] Jeong-Woo Lee, Dong-Jin Min, Jiyoun Kim, and Wonchan Kim, "A 600-dpi Capacitive Fingerprint Sensor Chip and Image-Synthesis Technique," *IEEE Journal of Solid-State Circuits*, Vol. 34, No. 4, April 1999, 469-475
- [11] Howard Demuth, Mark Beale, "Neural Network Toolbox For Use with MATLAB®," User's Guide Version 3.0, 1997 MathWorks, Inc., Natick, MA.
- [12] Jose. C. Principe, Neil R. Euliano, and W. Curt Lefebvre, "Neural and Adaptive Systems." John Wiley and Sons, 2000.
- [13] Lawrence O'Gorman, Stephanie C. Schuckers, Reza Derakhshani, and Lawrence Hornak; United States Patent, provisional application submitted on October 7, 1999.
- [14] Michael Schuckers, Personal Communications; WVU, March 2001.

Case	1	2	3	4	5	6	7	8	9	10	11	12
Live	0.9677	1.0000	1.0000	0.9085	1.0000	1.0000	1.0000	1.0000	1.0000	1.0000	1.0000	1.0000
Cadaver	-0.9928	-0.9922	-0.9732	-0.9938	-0.9885	-0.9841	-0.9514	-0.9923	-0.9849	-0.9903	-0.9940	-0.9836
Spoof	-0.9439	-0.9886	-0.9743	-0.9912	-0.9883	-0.9882	-0.9876	-0.9879	-0.9637	-0.9925	-0.9913	-0.9844

Table 1 Output of BPNN for training set.

Case	1	2	3	4	5	6
Live	1.0000	1.0000	1.0000	1.0000	0.9999	1.0000
Cadaver	-0.9950	-0.9944	-0.9890	-0.9938	-0.9852	-0.9827
Spoof	-0.9906	-0.9949	-0.9939	-0.8404	-0.9747	-0.9852

Table 2 Output of BPNN for test set.

Measure	EER (Live vs. Spoof)	EER (Live vs. Cadaver)
SM	11.11%	5.56%
DM1	22.22%	27.78%
DM2	11.11%	22.22%
DM3	16.67%	38.89%
DM4	22.22%	27.78%

Table 3 Equal error rates for all introduced measures. EER is the value at which FAR=FRR [14].

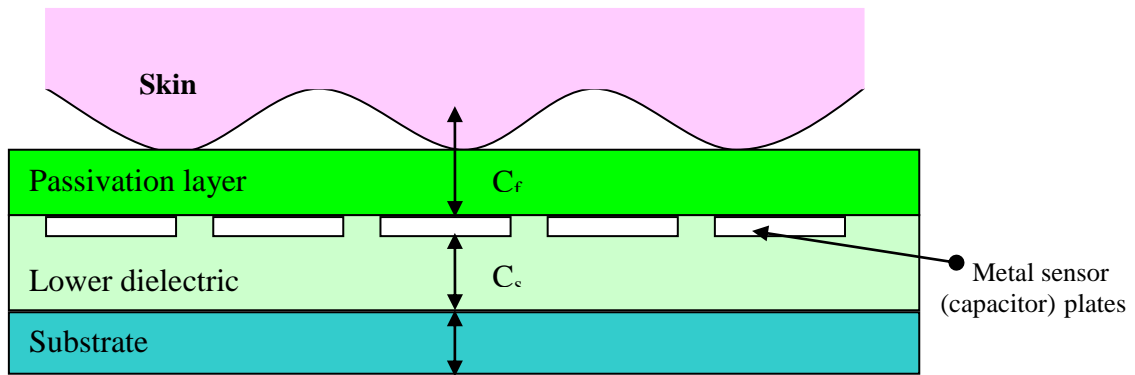


Figure 1 Typical capacitive sensor architecture



Figure 2 Live fingerprint @ t=0 (left) and @ t=5 (right)

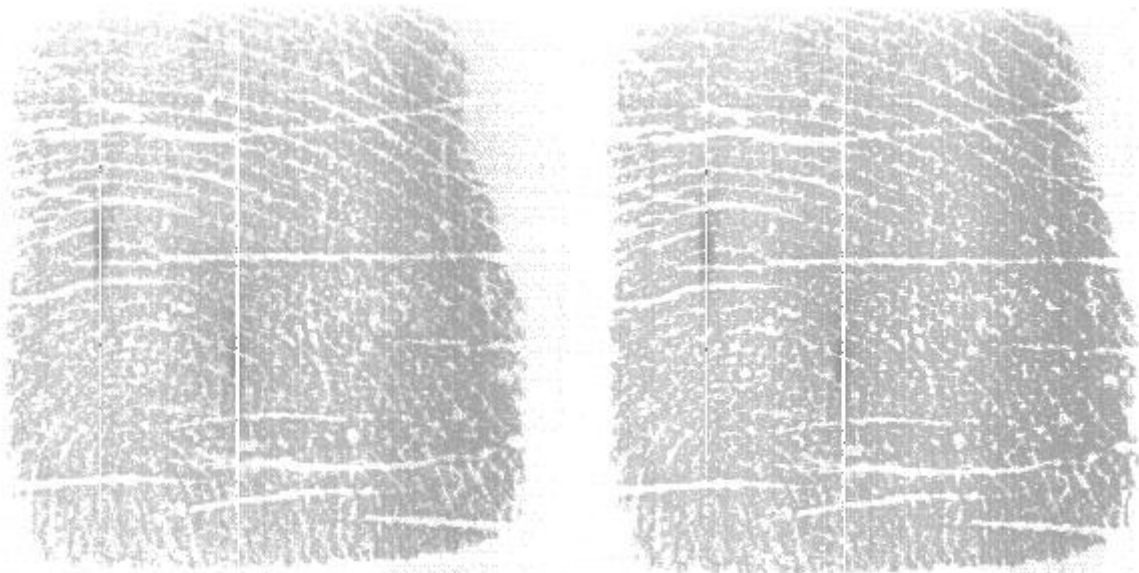


Figure 3 The first (left) and last (right) scan of a cadaver fingerprint.



Figure 4 The first (left) and last (right) scan of a spoof fingerprint.



Figure 5 Original scan (top left), blank scan (top right) and scan after noise and defects removed (bottom left), and binary image (bottom right).



Figure 6 Fingerprint ridges as found by steps 4, 5, and 6 overlaid on the fingerprint image

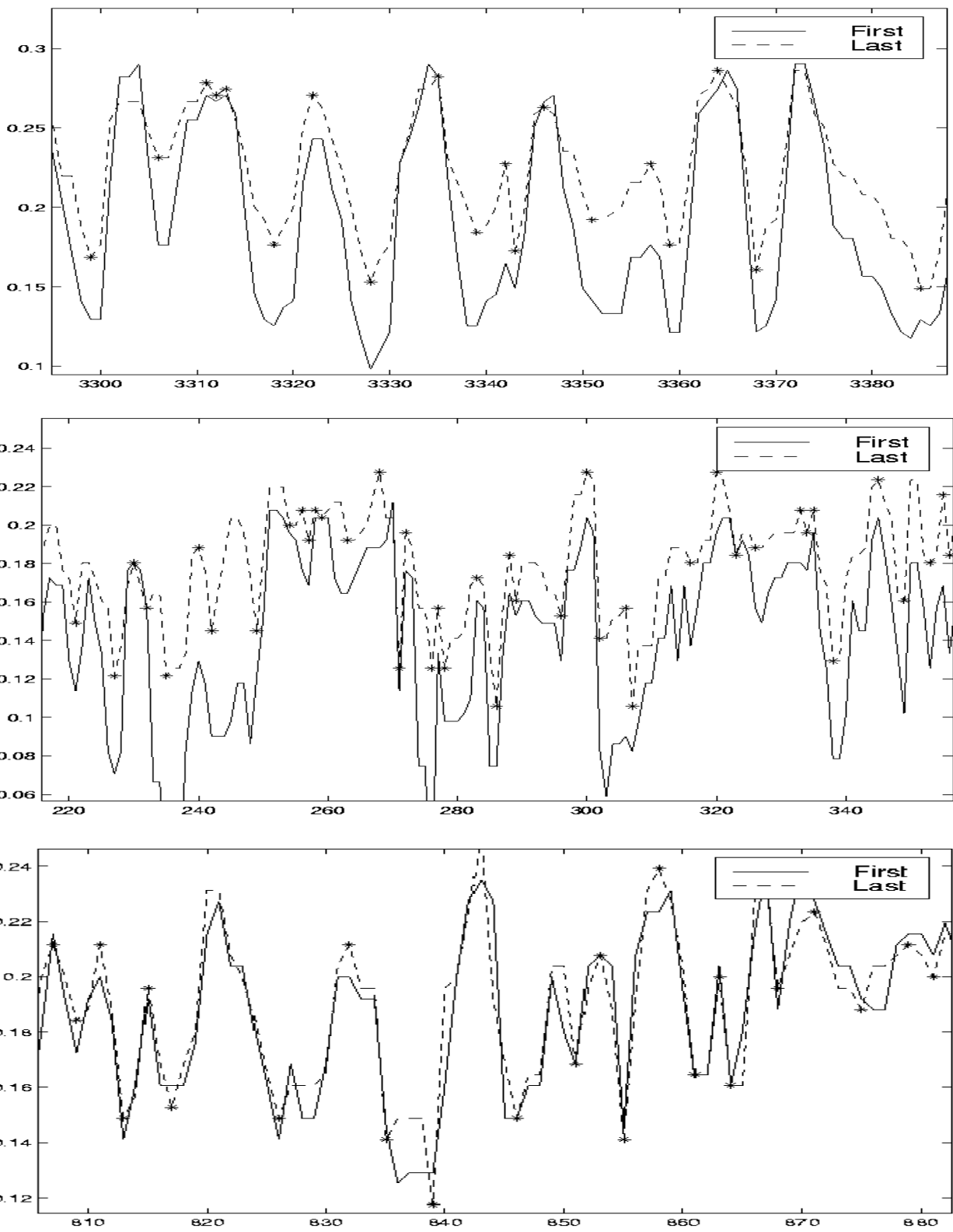


Figure 7 Portion of a live (top), cadaver (middle), and spoof (bottom) fingerprint signals.

* denotes minimums and maximums.

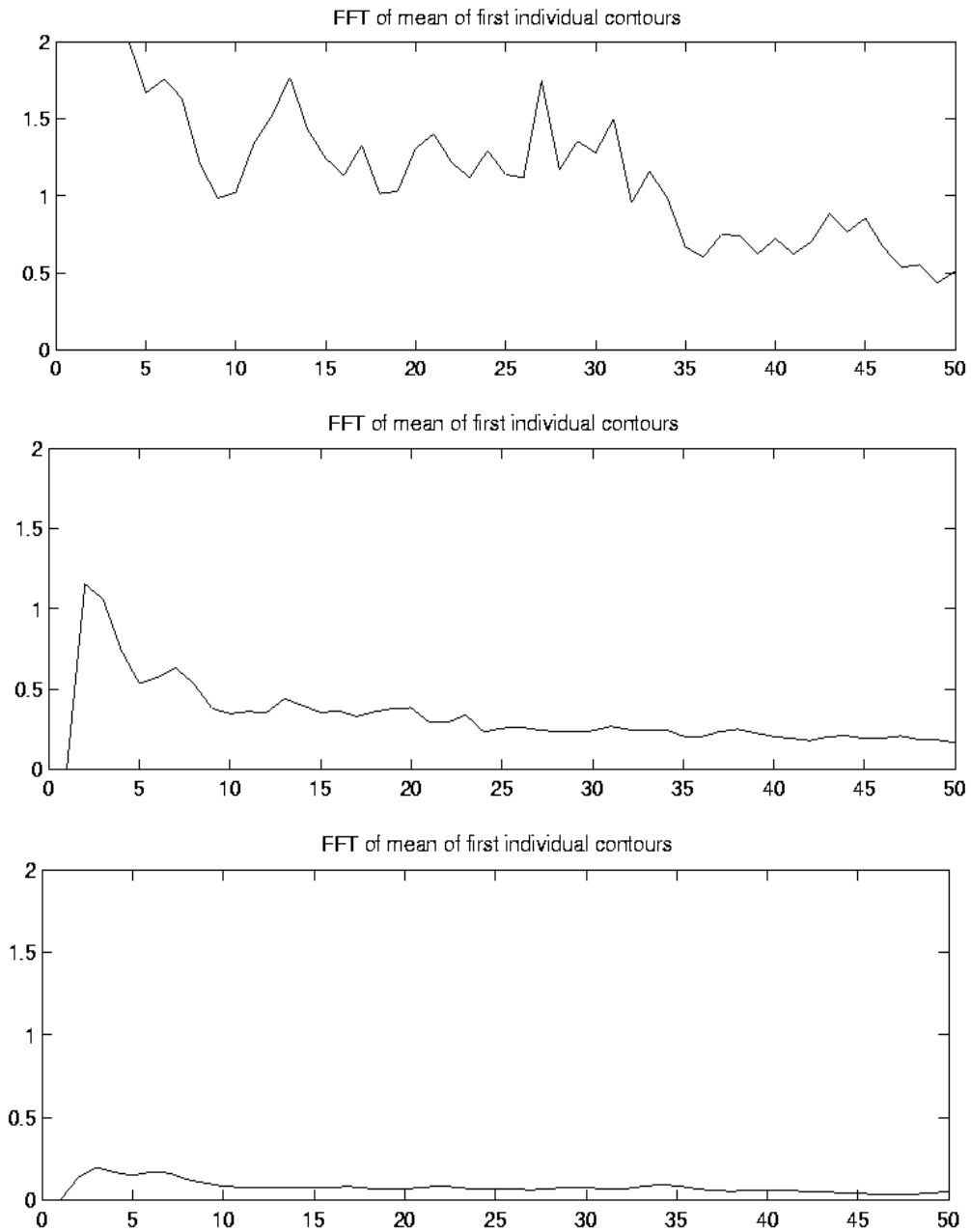


Figure 8 Average FFTs calculated from signal segments from the live (top), cadaver (middle), and spoof (bottom) capture of the fingerprints shown in Figure 2, 3, and 4 respectively.

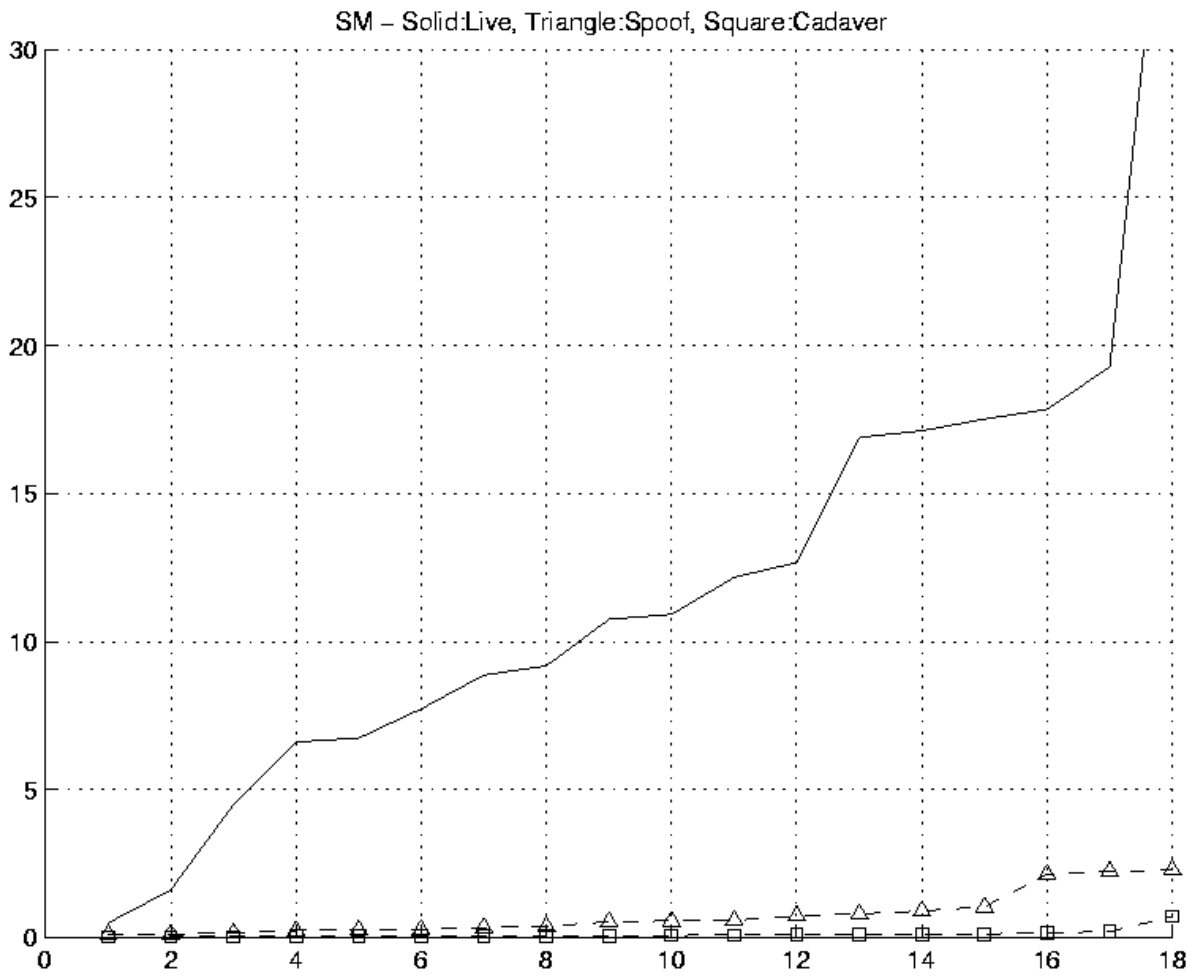


Figure 9 Static measure (SM), energy corresponding to 0.4-1.2mm pore separations. Legend - live: solid, spoof: triangle, and cadaver: square.

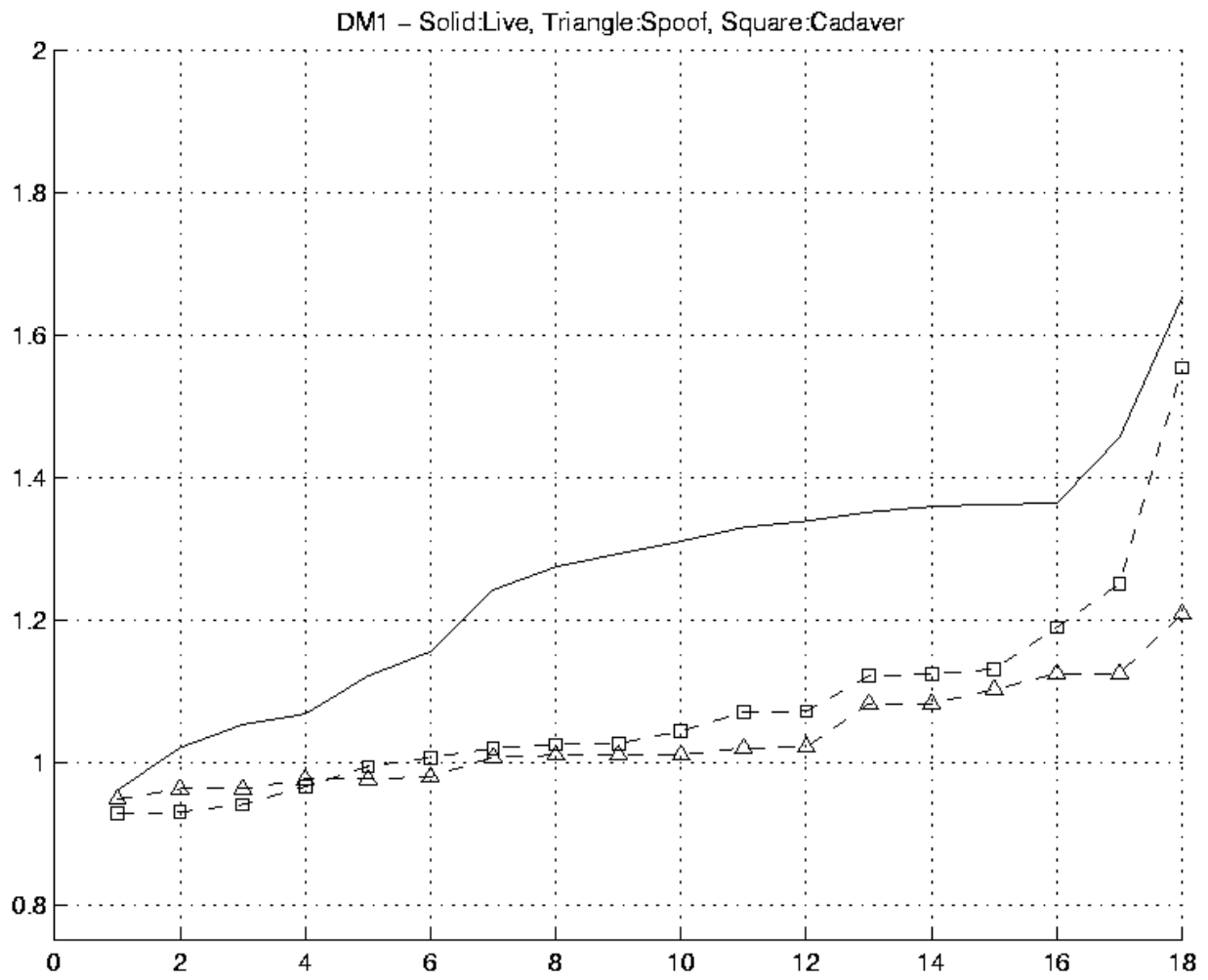


Figure 10 Dynamic measure 1 (DM1), First/last total swing ratio. Legend - live: solid, spooof: triangle, and cadaver: square.

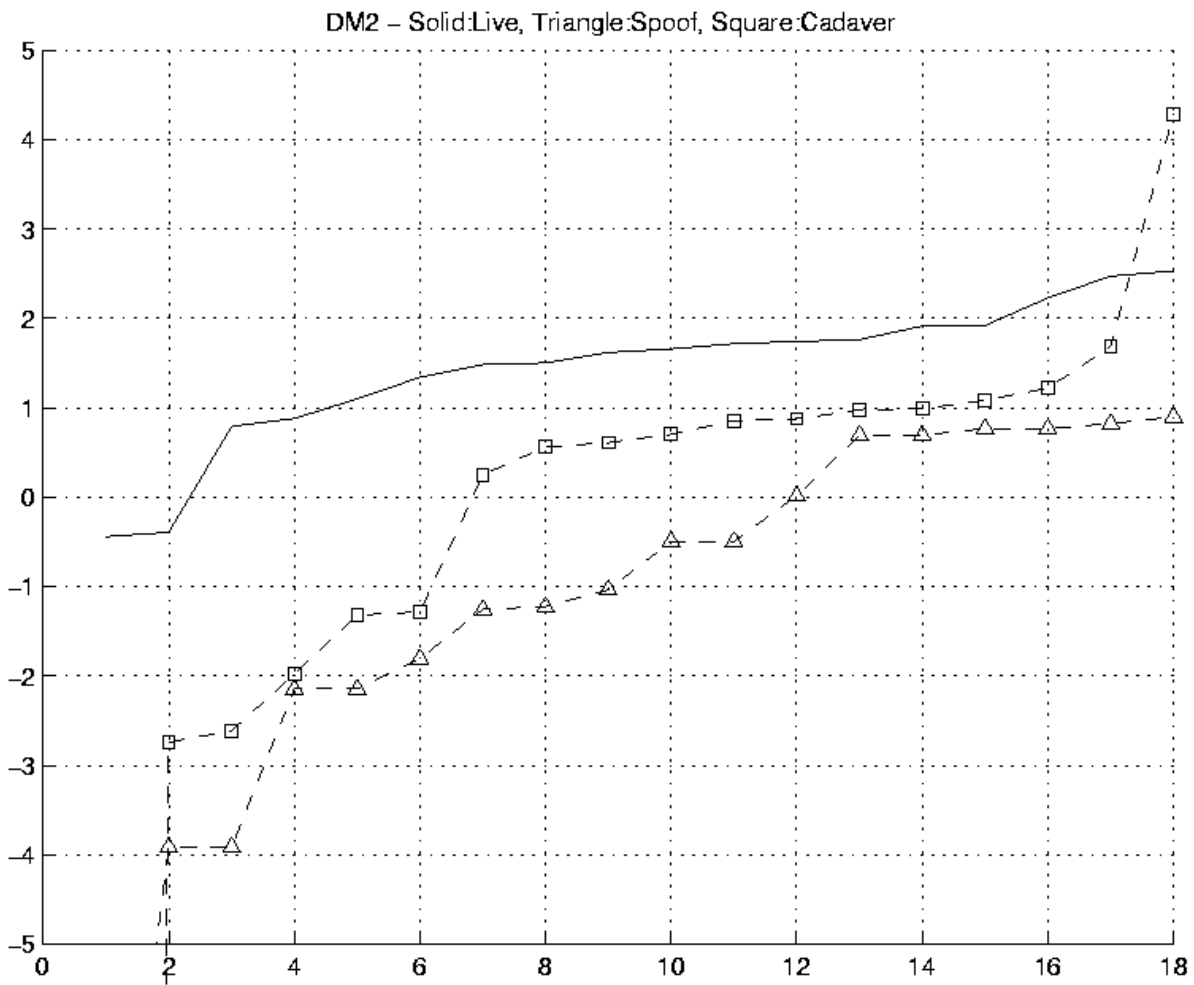


Figure 11 Dynamic measure 2 (DM2), min/max growth ratio. Legend - live: solid, spoof: triangle, and cadaver: square.

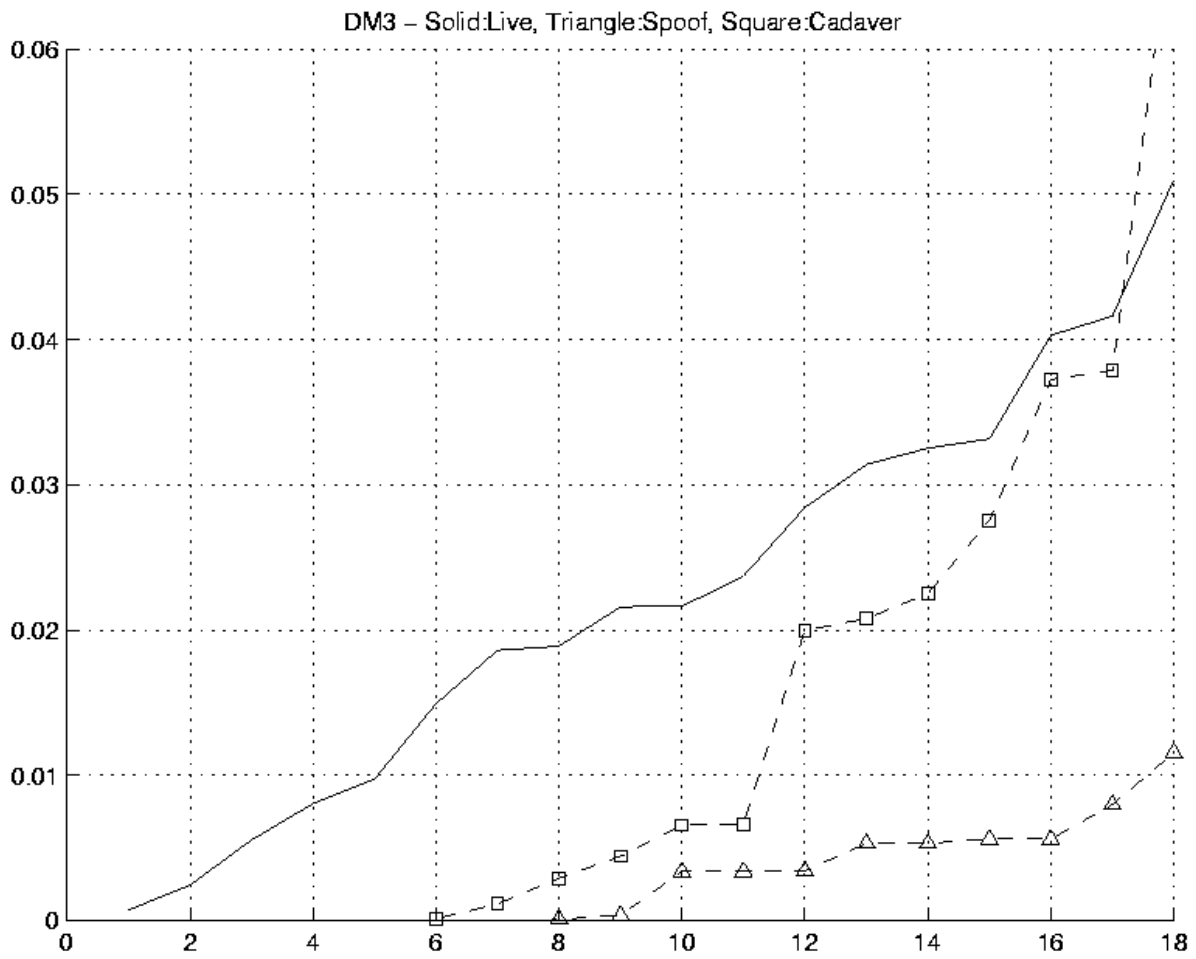


Figure 12 Dynamic measure 3 (DM3), mean of last minus first signals. Legend - live: solid, spooF: triangle, and cadaver: square.

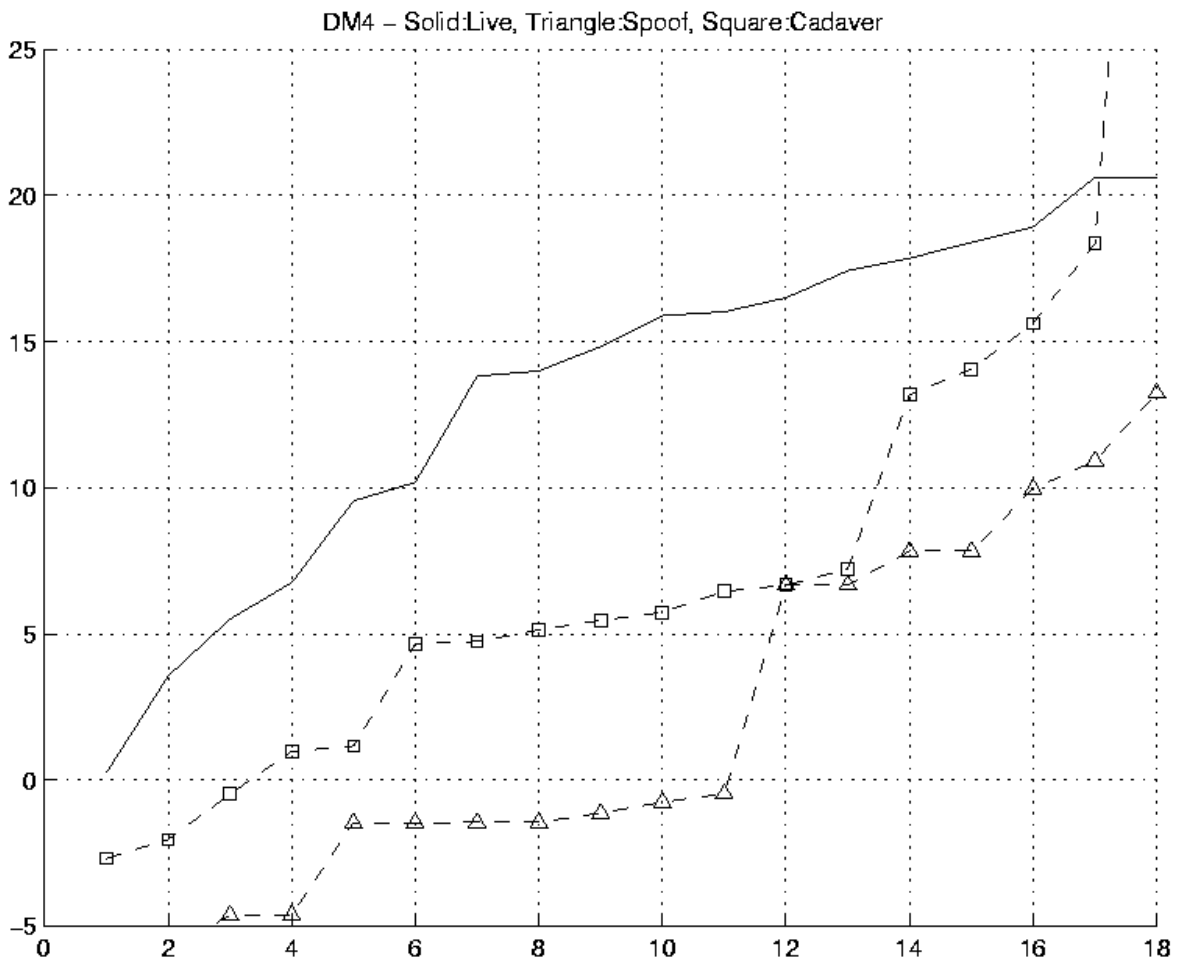


Figure 13 Dynamic measure 4 (DM4), percent change between last first signal standard deviations. Legend - live: solid, spoof: triangle, and cadaver: square.

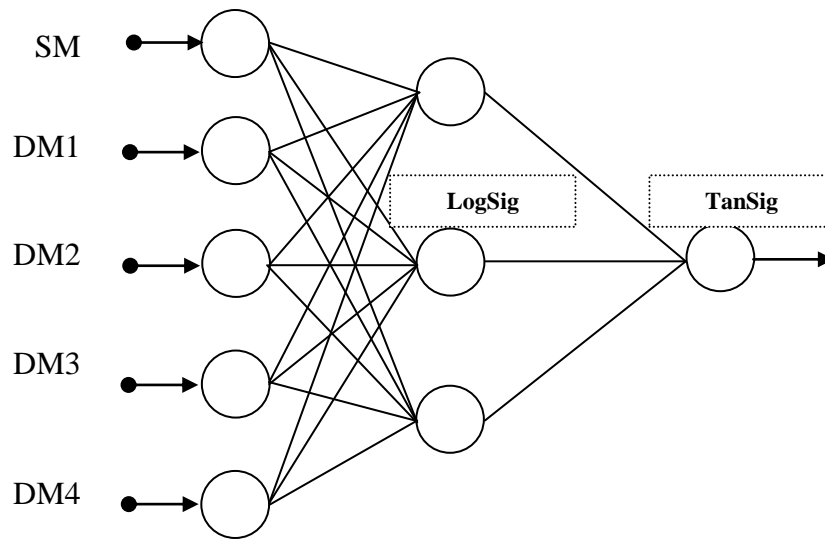


Figure 14 Layout of the back-propagation neural network. The inputs are the four dynamic and one static feature. Outputs (close to) +1 or -1 denote live or cadaver/spoof, respectively.

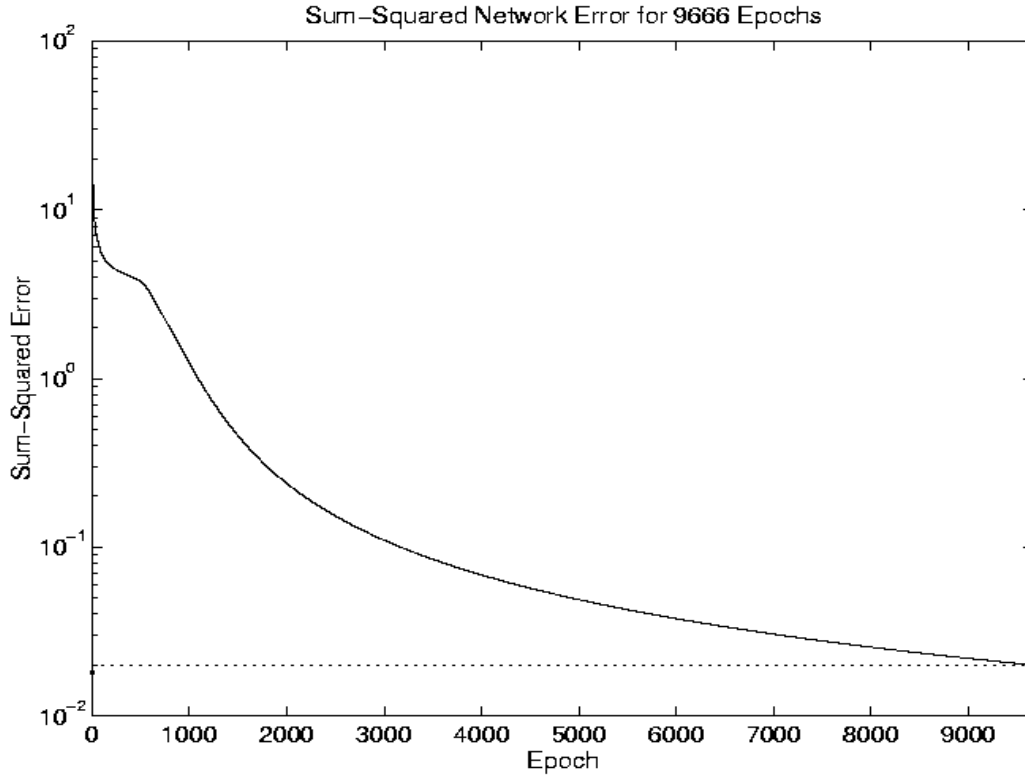


Figure 15 Plot of the sum-squared error during training. Error limit is set to 0.02. The number of epochs required for training was 9666.